

# Growing sabers: Mandibular shape and biomechanical performance trajectories during the ontogeny of *Smilodon fatalis*

Narimane Chatar<sup>1,2</sup>  | Romain Boman<sup>3</sup>  | Valentin Fischer<sup>1</sup>  |  
Valentina Segura<sup>4</sup>  | Clara Julémont<sup>1</sup> | Z. Jack Tseng<sup>2,5</sup> 

<sup>1</sup>Evolution and Diversity Dynamics Lab, UR Geology, Université de Liège, Liège, Belgium

<sup>2</sup>Functional Anatomy and Vertebrate Evolution Lab, Department of Integrative Biology, University of California, Berkeley, California, USA

<sup>3</sup>Department of Aerospace and Mechanical Engineering, Non-Linear Computational Mechanics (MN2L) Research Group, Université de Liège, Liège, Belgium

<sup>4</sup>Unidad Ejecutora Lillo, Consejo Nacional de Investigaciones Científicas y Técnicas (conicet)–Fundación Miguel Lillo, San Miguel de Tucumán, Argentina

<sup>5</sup>University of California Museum of Paleontology, Department of Integrative Biology, University of California, Berkeley, California, USA

## Correspondence

Narimane Chatar, Evolution and Diversity Dynamics Lab, UR Geology, Université de Liège, 4000 Liège, Belgium; Functional Anatomy and Vertebrate Evolution Lab, Department of Integrative Biology, University of California, Berkeley, CA 94720, USA.

Email: [narimane.chatar@uliege.be](mailto:narimane.chatar@uliege.be)

## Funding information

Fonds De La Recherche Scientifique - FNRS, Grant/Award Number: MIS F.4511.19; Fonds pour la Formation à la Recherche dans l'Industrie et dans l'Agriculture, Grant/Award Number: FC 36251; Belgian American Educational Foundation (BAEF); National Science Foundation (NSF), Grant/Award Number: DBI 2128146

## Abstract

The evolution of organisms can be studied through the lens of developmental systems, as the timing of development of morphological features is an important aspect to consider when studying a phenotype. Such data can be challenging to obtain in fossil amniotes owing to the scarcity of their fossil record. However, the numerous remains of Rancho La Brea allow a detailed study of the postnatal changes in an extinct sabertoothed felid: *Smilodon fatalis*. Despite numerous previous studies on the ontogeny of *Smilodon*, an important question remained open: how did the cubs of *Smilodon* acquire and process food? By applying 3D geometric morphometrics and finite element analyses to 49 mandibles at various developmental stages (22 of *S. fatalis*, 23 of *Panthera leo*, and 4 of early diverging felids), we assess the changes in mandibular shape and performance during growth. Both lions and sabertooths exhibit a shift in mandibular shape, aligning with eruption of the lower carnassial. This marks the end of weaning in lions and suggests a prolonged weaning period in *S. fatalis* owing to its delayed eruption sequence. We also highlight distinct ontogenetic trajectories, with *S. fatalis* undergoing more postnatal mandibular shape changes. Finally, although *S. fatalis* appears more efficient than *P. leo* at performing an anchor bite, this efficiency is acquired through ontogeny and at a quite late age. The delayed shape change compared with *P. leo* and the low

This is an open access article under the terms of the [Creative Commons Attribution-NonCommercial-NoDerivs](https://creativecommons.org/licenses/by-nc-nd/4.0/) License, which permits use and distribution in any medium, provided the original work is properly cited, the use is non-commercial and no modifications or adaptations are made.

© 2024 The Author(s). *The Anatomical Record* published by Wiley Periodicals LLC on behalf of American Association for Anatomy.

biting efficiency during the growth in *Smilodon* could indicate an extended duration of the parental care compared with *P. leo*.

#### KEYWORDS

Felidae, finite element analysis, geometric morphometric, mandible, ontogeny

## 1 | INTRODUCTION

The timing of the development of morphological features is an important aspect to consider even when studying adult phenotypes because changes in these timings (e.g., heterochrony) can result in divergent adult morphologies (Alberch, 1980; Alberch et al., 1979; Gould, 1985). The evolution of organisms should thus be regarded as the evolution of developmental systems (Waddington, 1975). Therefore, understanding ontogeny of organisms can allow us to better understand the assembly of their peculiar Baupläne. Such research programs also provide insights into the selective forces at play during the different ontogenetic stages of a given taxon.

One recurring peculiar trait amongst continental vertebrate predators is the development of saber-like upper canines. It evolved in various groups, from placental and marsupial mammals to gorgonopsians and creodonts (*sensu lato*) (Anton, 2013; Emerson & Radinsky, 1980; Turner et al., 2011; Van & Jenkins, 2002). Still, the most iconic sabertooth taxon is probably *Smilodon fatalis* thanks to its abundant fossil record at Rancho La Brea (California, USA); this sample offers an unprecedented window to better apprehend its behavior, life history, and evolution (Akersten, 1985; Binder et al., 2016; Emerson & Radinsky, 1980; Feranec, 2004; Hartstone-Rose et al., 2012; Merriam & Stock, 1932; Van et al., 2009; Werdelin et al., 2018). Although research into the ontogeny of most fossil taxa is notoriously difficult owing to the scarcity of an adequate fossil record, it is not the case in the Rancho La Brea, which consist of asphalt deposits acting as a natural trap that are known to contain an incredibly well preserved Late Pleistocene fossil assemblage, the preservation is impressive both in terms of the amount but also the stage of each specimen (Merriam & Stock, 1932; Stock, 1930). The numerous remains from Rancho La Brea allow a detailed study of the post-natal changes in *S. fatalis*, which is even more impressive knowing that predator remains are generally scarcer. Mammalian carnivores usually represent about 10% of the mammalian biomass in modern ecosystems, a proportion typically reflected in the fossil record (Eisenberg, 1981; Klein & Cruz-Urbe, 1987; Stock & Harris, 1992).

All felids (rather they possess elongated upper canines or not) undergo dramatic changes in diet from suckling to a carnivorous diet that is highly demanding

from a mechanical standpoint (Christiansen, 2007; Segura et al., 2017). The transition between these vastly different feeding modes was probably even more drastic in extreme sabertoothed taxa such as *Smilodon*, considering its peculiar hunting method (Akersten, 1985; Turner et al., 2011). Some aspects of the development of *S. fatalis* are already well known. For instance, dental wear evolves differently during growth between *S. fatalis* and *Panthera leo*: incisors and lower canines of the extant lion exhibit stronger wear while the strongest wear is located in post canine teeth in *Smilodon* (Tejada-Flores & Shaw, 1984). This could mean that the hypertrophy of the canines in *Smilodon* mechanically drives the use, and wear of the teeth. The growth rate of the upper canines has also been investigated through the analysis of carbon and oxygen isotopes within the enamel. These data revealed that the sabers of *S. fatalis* grew approximately by 80 mm over a 12-month period, translating into a growth rate of 7 mm per month (Feranec, 2004). Hence, sabers in *Smilodon* formed through a combination of rapid growth and sustained development over an extended duration (Feranec, 2004). Christiansen (2012) noted that cub skulls of *Smilodon* underwent much more ontogenetic changes than pantherine cubs, such as stronger posterodorsal displacement of the face and a stronger enlargement of the mastoid process (Christiansen, 2012). Finally, it is known that *S. fatalis* wore both its deciduous and permanent upper canines for a quite long period of time and that young adults fully grow their permanent sabers at the age of 34–41 months (Wysocki et al., 2015). This combination of unusual dental wear, rapid cranial ontogenetic changes, and delayed eruption of the permanent sabers, combined with a rather long double-fanged phase, leaves a question open: how did *Smilodon* cubs acquire and process food?

Complete skulls of juvenile *Smilodon* are uncommon: out of the 2100 *S. fatalis* specimens from Rancho La Brea that Miller (1968) studied, only nine are nearly complete juvenile skulls (Miller, 1968). The reason for this rarity has been speculated to be the presence of streams in the asphalt (Harris, 2015) dislocating skulls with incomplete fusion of the sutures. Also, extant felids tend to hide their cubs while hunting, which could have prevented many juvenile *Smilodon* from being preserved in the tar pits in the first place. By comparison, complete mandibles or hemimandibles were much more common in the

collections of the Natural History Museum of Los Angeles County and allowed us to sample a complete ontogenetic sequence of *S. fatalis* (17 juveniles and 5 adults) using 3D geometric morphometrics and finite element analysis. We looked for potential shifts in the mandibular shape of *S. fatalis* related to a change of diet (from a milk-based to a meat-based diet) or linked to the double-fanged phase (e.g., Tseng, 2024). More precisely, in this study, we aim to answer the following questions:

1. Does the drastic change of diet have an impact on the mandibular shape of *S. fatalis*?
2. Do sabertoothed felids undergo more ontogenetic changes in their mandible than extant big cats?
3. Is there a shift in the mechanical performance of *S. fatalis* that could indicate the ability to hunt on their own?

To do so, we used the extant lion (*P. leo*) for comparison, as the different stage of its growth are well known and understood (Smuts et al., 1978). We quantified the ontogenetic mandibular shape trajectories of both species and quantified the mechanical behavior of their mandibles using finite element analysis to look for potential variation in shape-performance relationships through ontogeny.

## 2 | MATERIALS AND METHODS

### 2.1 | Material

A total of 49 mandibles were used to perform the analyses. Specimens were considered adult when their full set of permanent teeth had fully erupted, all the others were considered juvenile. Twenty-two mandibles of *S. fatalis* (17 juveniles and 5 adults) from the La Brea Tar Pits and Museum (Los Angeles) as well as 20 mandibles of *P. leo* (18 juveniles and 2 adults) from the Muséum National d'histoire Naturelle (Paris, France) and the Royal Museum of Central Africa (Tervuren, Belgium) were surface scanned using a Creaform HandySCAN 300 laser surface scanner, at a 0.2 mm resolution. Scans were processed using “VX models” (VX model, 2023). To complete our dataset, three additional specimens of *P. leo* (two adults and one juvenile) were downloaded from MorphoSource and Digimorph (see Table S1 for specimen list and institution details). *P. leo* was chosen for comparison as it represents a large-bodied felid and its ontogeny has already been thoroughly studied (Segura et al., 2017; Smuts et al., 1978; Wirkner et al., 2022). All the 3D models associated with this project are available on Morphosource (Project ID: 000599525, <https://www.morphosource.org/>

[projects/000599525](https://www.morphosource.org/projects/000599525)). We computed topological deviation to visualize the differences between juvenile and adult specimens, in both taxa. To do so, we aligned and scaled the models using GeoMagic Wrap; the deviation is reported as the shortest distance from the test model to any point on the reference model. We also include 3D models of a series of early diverging, plesiomorphic taxa for some analyses: *Proailurus lemanensis* and *Pseudaelurus intrepidus* from the Smithsonian National Museum of Natural History (Washington) as well as *Pseudaelurus marshi* and *Pseudaelurus skinneri* from the American Museum of Natural History (New York).

### 2.2 | Geometric morphometrics

We placed 6 type-II landmarks (Bookstein, 1991) and 3 curves for a total of 22 semi-landmarks on the mandible (Figure 1 and Table S2 and S3) using Stratovan Checkpoint v2018.08.07 (Stratovan Corporation, 2018) and exported the coordinates as “pts” files. All subsequent geometric morphometric and statistical analyses were performed in the R statistical environment (R Core Team, 2021). The landmark coordinates were imported into R using the custom function “import.pts” written by one of us (N.C.; <https://github.com/cha-nar/importpts>). Semilandmarks to slide were defined in a csv file (See Table S3) and a generalized procrustes superimposition was performed using the gpgen function from the geomorph package (Adams & Otárola-Castillo, 2013) specifying the semi landmarks to slide using the “curve” argument.

### 2.3 | Linear and angular measurements

In addition to the landmarks, five linear and one angular measurements were taken directly in “VX models” (VX model, 2023). Those measurements (Figure 1 and Table S1) represent either typically discussed sabertooth traits (the height of the coronoid process, the length of the diastema length and the inclination angle of the symphysis) or functional traits (the length of the cheek teeth row, the height of the mandibular body). Linear measurements were taken using the caliper tool. Angular measurements (inclination of the symphysis) were taken using the angular tool (VX model, 2023) that computes the angle between two planes. We created these planes by placing three points on the symphysis (right under the lower canine, approximately in the middle of the symphysis and at its base) and three points on the ventral border of the mandible (on the anterior portion at the junction with the symphysis, in the middle and on the angular process).

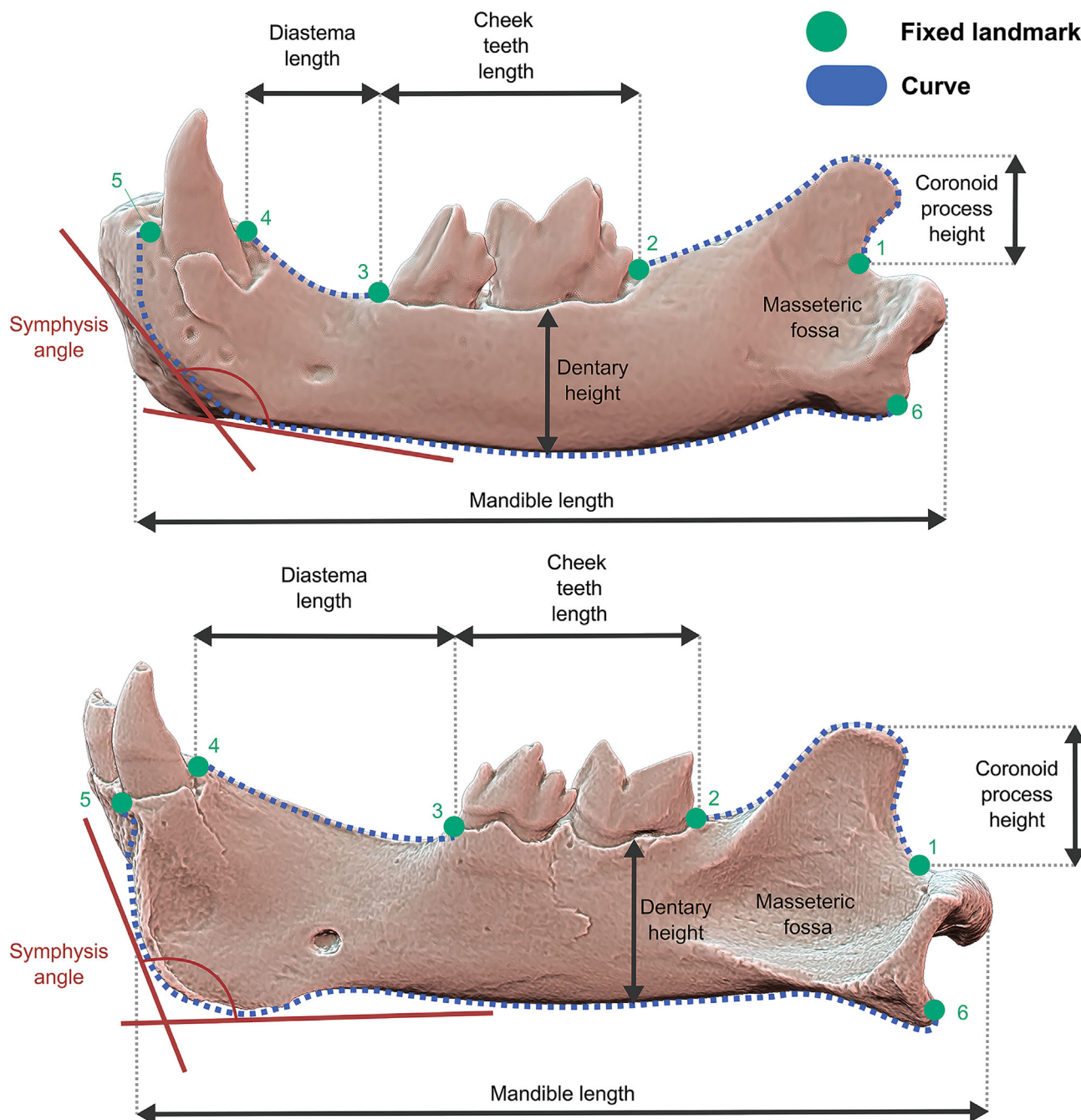


**FIGURE 1** Cub (LACM-HC-2002-L-4) and adult (LACM-HC-2002-HC-2002-2) mandible of *Smilodon fatalis*, showing the different landmarks and curves placed on each specimen as well as the linear (black) and angular (red) measurements taken. Not to scale. Not that “cheek teeth” include all post canine teeth, from the first premolar to the last molar present in the tooth row.

## 2.4 | Morphospaces and ontogenetic trajectories

A principal components analysis (PCA) was performed using the `gm.prcomp` function of the `geomorph` package (Adams & Otárola-Castillo, 2013). We looked at ontogenetic trajectories using the `plotAllometry` function of the `geomorph` package (Adams & Otárola-Castillo, 2013). To test the difference between the ontogenetic trajectories we used a permutational multivariate analysis of

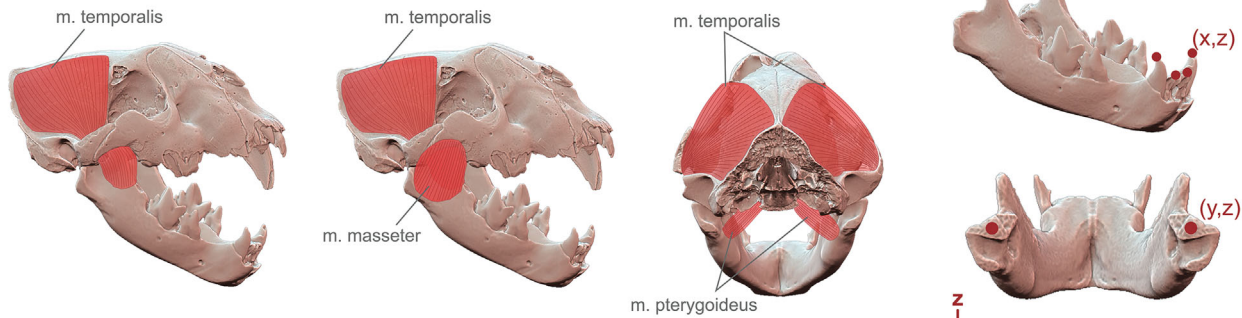
variance, with species, size, and species + size as factors using the “`adonis2`” function from the `vegan` package (Dixon, 2003). All our plots were performed using `ggplot2` from the `ggplot2` package (Wickham, 2016).

## 2.5 | Finite element analysis

Three muscle groups (*M. temporalis*, *M. masseter*, and *M. pterygoideus* groups) were drawn on each side of each



*Smilodon fatalis*, juvenile with a full set of milk teeth LACM-HC-2002-L-4



*Smilodon fatalis*, fully grown adult LACM-HC-2002-HC-2002-2

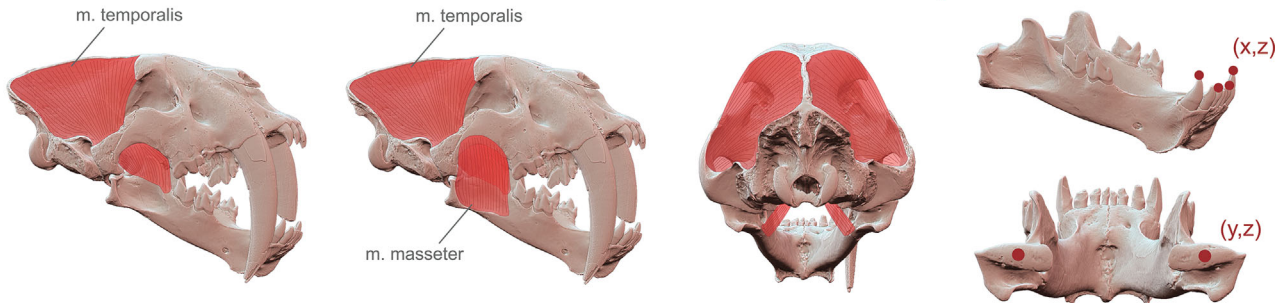


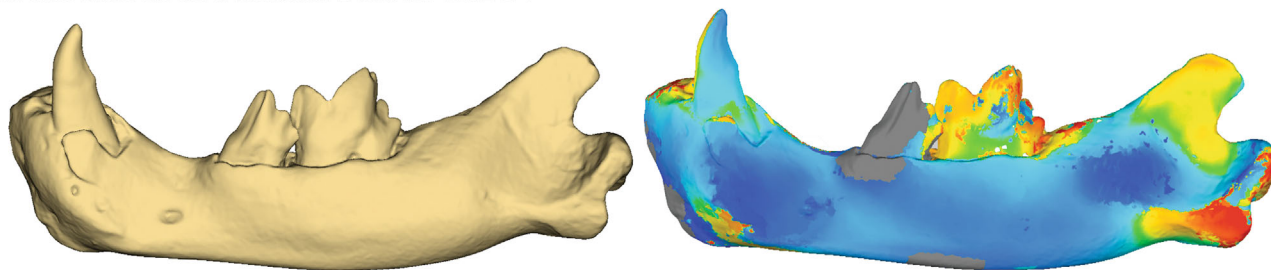
**FIGURE 2** Schematic reconstruction of the muscle used in the simulations and the constraints placed on the mandible for an adult (LACM-HC-2002-HC-2002-2) and a juvenile (LACM-HC-2002-L-4) specimen of *Smilodon fatalis*.

mandible (six muscle attachment regions in total) using GeoMagic following Chatar et al. (2022) (Figure 2). As associated juvenile skulls and mandibles were extremely scarce (only one specimen), the physiological cross-sectional area estimation would have been ambiguous to compute so we estimated the forces (in Newtons) pulling each muscle insertion by multiplying the insertion area (in  $\text{mm}^2$ ) by the maximum tension produced by mammalian muscle fibers ( $0.3 \text{ N/mm}^2$ ) (Dessem & Druzinsky, 1992). In order to simulate a “sabertooth killing bite” where the animal uses its mandible as an anchor on the throat of the prey, we used four nodal constraint points on the most anterior part of the mandible (Figure 2). A nodal constraint was also created on each mandibular condyle preventing any dorsoventral or rostrocaudal movement ( $x$ ,  $z$  axes) but still allowing a certain degree of bending of both sides of the mandible one toward the other in the mediolateral axis ( $y$  axis) (Figure 2). All mandibles were considered homogeneous isotropic linear elastic material; a Young’s modulus of 18 GPa and a Poisson’s ratio of 0.3 were defined according to (Erickson et al., 2002; Gill et al., 2014; Grosse et al., 2007).

For each specimen, mandible meshes were produced at three resolutions: 100,000, 200,000, and 300,000 triangles on the surface of the model, resulting in about 300,000, 850,000, and 1,500,000 tetrahedral elements, respectively. Analyses were run in Metafor following the protocol published by Chatar et al. (2023). Although analyses were

performed on the mandibles, articulation with a cranium is essential to run realistic muscle-induced simulation because it is important to correctly estimate muscular origins and orient the forces toward muscle insertions. Because associated skulls and mandibles are quite rare in juveniles, some mandibles had to be articulated with crania belonging to other specimens. Three juvenile crania of *S. fatalis* and four juvenile crania of *P. leo* were scanned and re-scaled to fit the mandibles when needed (See Tables S4 and S5 for the crania articulated with each mandible and the scaling factor we used). For model comparisons, we extracted three performance variables from the finite element simulations: a qualitative comparison of von Mises stress heatmaps (a scalar measure of the level of stress induced by the biting scenario), the mechanical efficiency (a scale-independent estimation of the muscle force proportion that is translated into bite force), and the internal energy (in mJ), which we scaled using the volume of each model to quantify the work of the external forces (later called “adjusted internal energy”). The exact number of triangles, tetrahedra, and raw data can be found in Table S6; averaged values and confidence intervals are available in Table S7. The subset selected for finite element simulations consisted of 13 specimens, comprising seven *S. fatalis* individuals (two adults and five juveniles) and 6 *P. leo* specimens (two adults and four juveniles). Each specimen underwent three analyses, corresponding to the three different resolutions, yielding a cumulative total of 49 simulations.

Juvenile with a full set of milk teeth LACM-HC-2002-L-4



Fully grown adult LACM-HC-2002-HC-2002-2

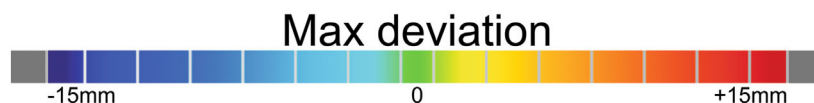
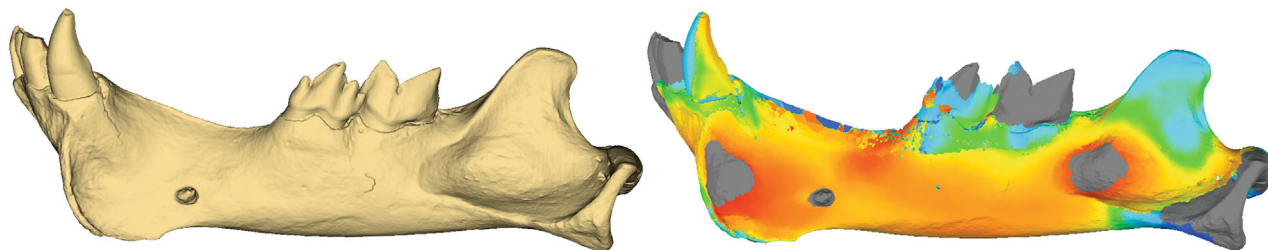


**FIGURE 3** Topological deviation in the mandible of *Smilodon fatalis* between a fully grown adult specimen (LACM-HC-2002-HC-2002-2) (bottom) and a juvenile (top) with a full set of milk teeth (LACM-HC-2002-L-4). Not to scale. Gray colors indicate values out of scale.

### 3 | RESULTS

#### 3.1 | Anatomical comparison

Our topological deviation maps (Figure 3) show that the mandibular body appears to be the region undergoing most of the post-natal ontogenetic changes. The most obvious changes are the following: a global straightening of the ventral border of the mandible, an elongation of the diastema, the development of the mental process, and a rotation of the symphyseal region posteriorly in the transverse plane making it appear more vertical. The masseteric fossa also gets deeper during the growth while the coronoid process rotates anteriorly: it is vertical in adults while it is projected posteriorly in juveniles. The mandibular condyle and angular process also concentrate important change, increasing in dorsoventral height and displacing ventrally throughout ontogeny. In juvenile specimens the angular process is higher than the ventral border of the mandible while it is perfectly aligned with the ventral border in adults.

Interestingly, when compared side to side with *P. leo*, the mandibular body of a cub of *S. fatalis* resembles that of the extant lion cub (Figure 4). The cubs of both species share a curved and well-developed dorsoventrally, with the posterior part of the dentary being elevated compared

with the anterior section. The masseteric fossa starts more anteriorly in adults than in juveniles in both species. Juveniles also show a more developed mandibular condyle than in adult of the same species; the mandibular condyle remains quite well developed in *S. fatalis* while it is thin in adult specimens of *P. leo* relative to the size of the mandible. The ascending ramus is already quite variable in both species with cubs of *S. fatalis* already showing a short coronoid process while that of *P. leo* is already high and projected posteriorly. The two mental foraminae of *P. leo* cubs are much larger than in adults while the unique mental foramen of *S. fatalis* cubs is smaller than in adult specimens.

Globally, from basic side-by-side comparisons, *S. fatalis* seemingly undergoes more post-natal ontogenetic changes in mandibular shape than the extant lion. However, to confirm this observation, statistical tests are still required (see the following sections).

#### 3.2 | Species-specific morphospace occupation through ontogeny

Our PCA on the geometric morphometric shape data for *S. fatalis* retrieved 19 axes, the first two explaining a total of 51.35% of data variance (30.64% and 20.71%,

## Juveniles



*Panthera leo*



*Smilodon fatalis*



## Adults

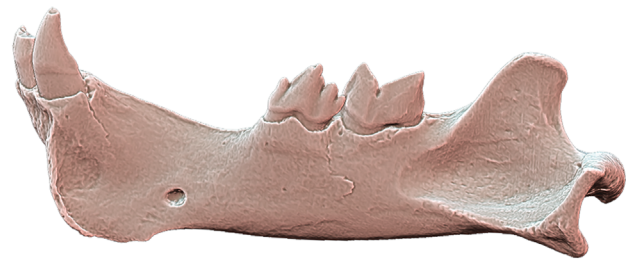


**FIGURE 4** Comparison of the mandible in lateral view of juvenile (left) and adult specimens (right) of *Panthera leo* (top) and *Smilodon fatalis* (bottom). Not to scale.

respectively) (Figure 5a). This morphospace highlights a clear differentiation between two ontogenetic stages: cubs with a full set of milk teeth (Low PC1 and High PC2), and cubs showing an erupting m1 (average to high PC1 and low to high PC2). Additionally, four of our specimens with a full permanent dentition (LACM-HC-2002-2, LACM-HC-2002-32, LACM-HC-2002-44, LACM-HC-2002-66, see Figure S1 for morphospaces with specimen numbers) also seem to be separated from both an outlying adult and the cubs with erupting m1 (High PC1 and high PC2). An outlying specimen clustering with the juvenile specimens (LACM-HC-2002-125, see Figure S1) shows a quite curved mandibular body, which is unusual in adults of *S. fatalis* and indeed similar to what is observed in young cubs. There is a marked allometric component on PC1 with smaller specimens occupying the lowest values, those values increasing alongside the log corrected centroid size.

The PCA on the geometric morphometric shape data on the *P. leo* retrieved 21 axes, the first two explaining a total of 57.76% of data variance (42.17% and 15.59%, respectively) (Figure 5b). On the first axis, there is a clear differentiation between two different ontogenetic stages: specimens with the m1 (lower carnassial) not yet erupted

occupy higher values along PC1 (shorter diastema, dorsoventrally thicker mandibular body, and more curved mandibular body) while specimens with an erupted lower carnassial occupy the lowest values of the PC1 (longer diastema, straighter coronoid process, and a dorsoventrally thinner mandibular body). Specimens are well spread along PC2 and there is no apparent ontogenetic trend on this axis.

### 3.3 | Comparison of the mandibular shape variation in both species

Our common PCA on the whole shape dataset retrieved 45 axes, the first two explaining a total of 51.35% of data variance (respectively 30.64% and 20.71%) (Figure 6). PC1 discriminates *S. fatalis* from the other felids in the dataset, occupying negative values while the other felids exhibit positive values. One exception is *Proailurus lemanensis* which shows similar PC1 values to the smallest cubs of *S. fatalis* on this axis, and is the only specimen with PC2 values lower than  $-0.05$  on this axis. Whereas, cubs in both species appear relatively close to an early diverging felid mandibular shape (*Pseudaelurus* spp.),

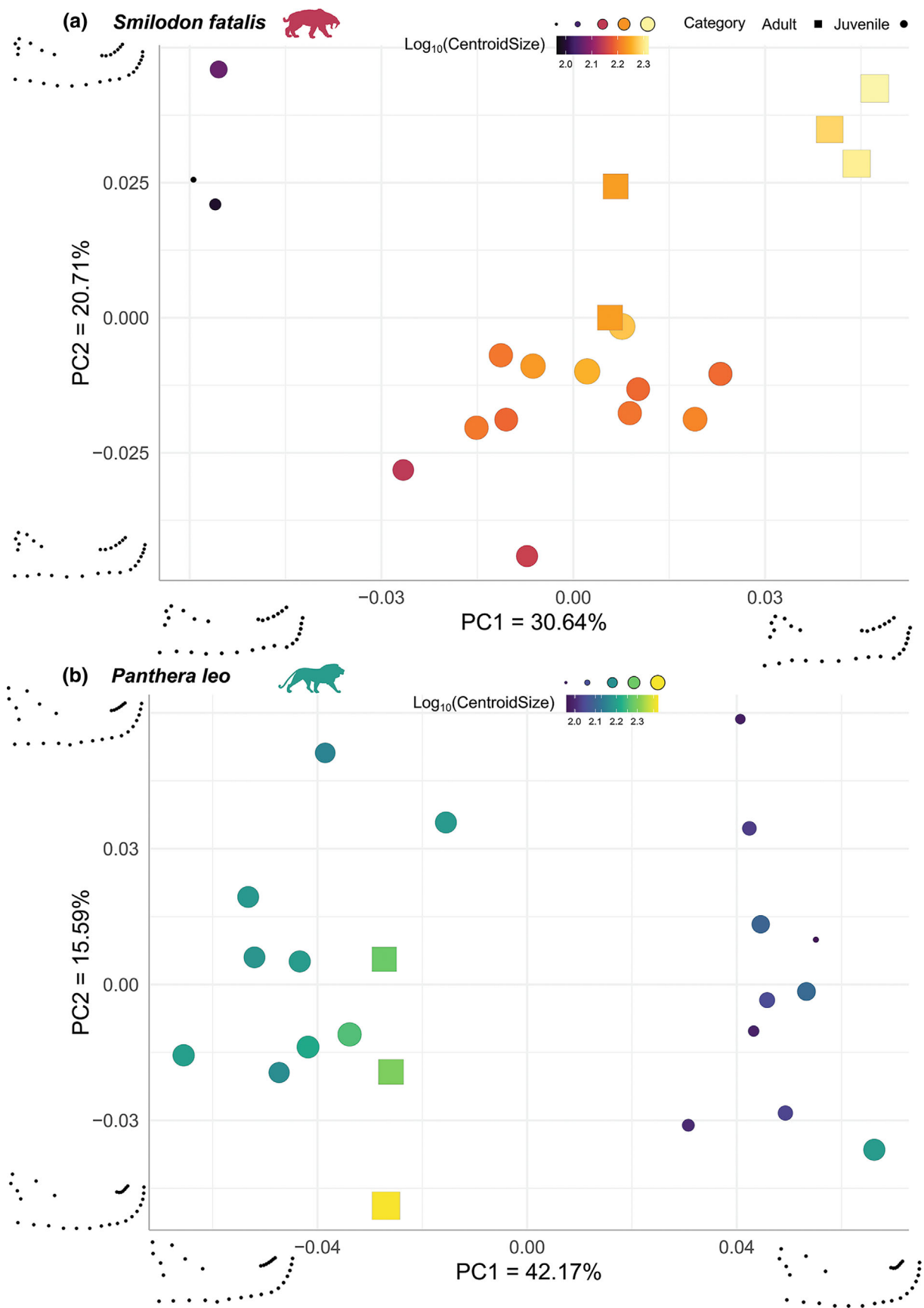
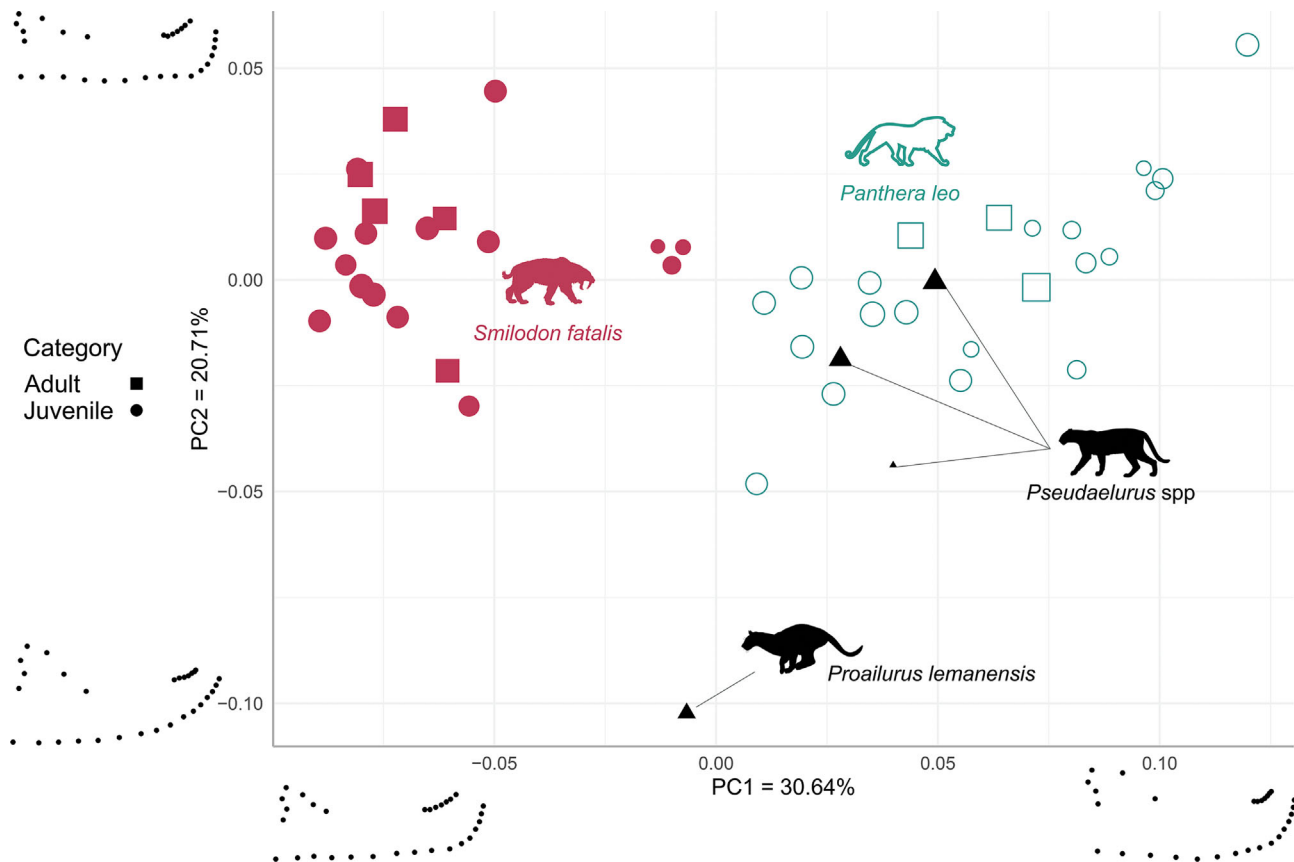


FIGURE 5 Per species morphospace occupation of (a) *Smilodon fatalis* and (b) *Panthera leo*. See Figure S1 for specimen numbers.





**FIGURE 6** Morphospace occupation of felid mandible shapes. Point size is relative to the log-transformed centroid size of each individual.

adult lions remain confined close to this area of the morphospace while adult *Smilodon* explore the lowest values of the PC1. Overall, *P. leo* occupies a larger proportion of the morphospace than *S. fatalis* despite a similar sample size (20 mandibles of *S. fatalis* and 22 mandibles of *P. leo*). This pattern holds even after considering the size gap between the three smallest specimens of *S. fatalis* and the other specimens which could be owing to an incomplete sampling of transient ontogenetic stages given the fragmentary fossil record.

To explore growth-related changes, we computed the ontogenetic allometric trajectories using the first principal component of the predicted values of the multivariate regression of shape (landmark coordinates) on size (Log centroid size) (Figure 7) obtained from the plotAllometry function of the geomorph package (Adams & Otárola-Castillo, 2013), as it is an effective way to plot ontogenetic variation when dealing with landmark coordinates (Mitteroecker et al., 2004). Regression scores of mandibular shape versus log-transformed centroid sizes can be found in Figure S2. Juveniles appear slightly more similar to one another than adults between the two species (see the arrows indicating distances between cubs and adults in

Figure 7), which is coherent with our anatomical observations detailed above (see Figure 4). There is a significant difference in slopes between both taxa ( $p$ -value = 0.001). The slope of the ontogenetic trajectories is more pronounced in *S. fatalis* (slope  $-0.015$ , intercept  $-0.005$ ) than in *P. leo* (slope  $-0.0057$ , intercept  $0.078$ ), confirming that *S. fatalis* underwent more post-natal mandibular changes than *P. leo*.

### 3.4 | Evolution of typical saber-tooth traits during the ontogeny

A few of the linear measurements taken on the same set of specimens follow similar trends in both species (Figure 8 and S3 and S4). The most striking is the dorso-ventral height of the dentary, which shows the same trends but also similar values at similar stages of development for both species (Figure 8c and S2C). The length of the cheek tooth row is comparable in older juveniles but much greater in smaller cubs of *S. fatalis* and in similar-sized cubs of *P. leo*; this measurement tends to be smaller in adult *Smilodon* than in adult lions (Figure 8a, S3A and S4A).

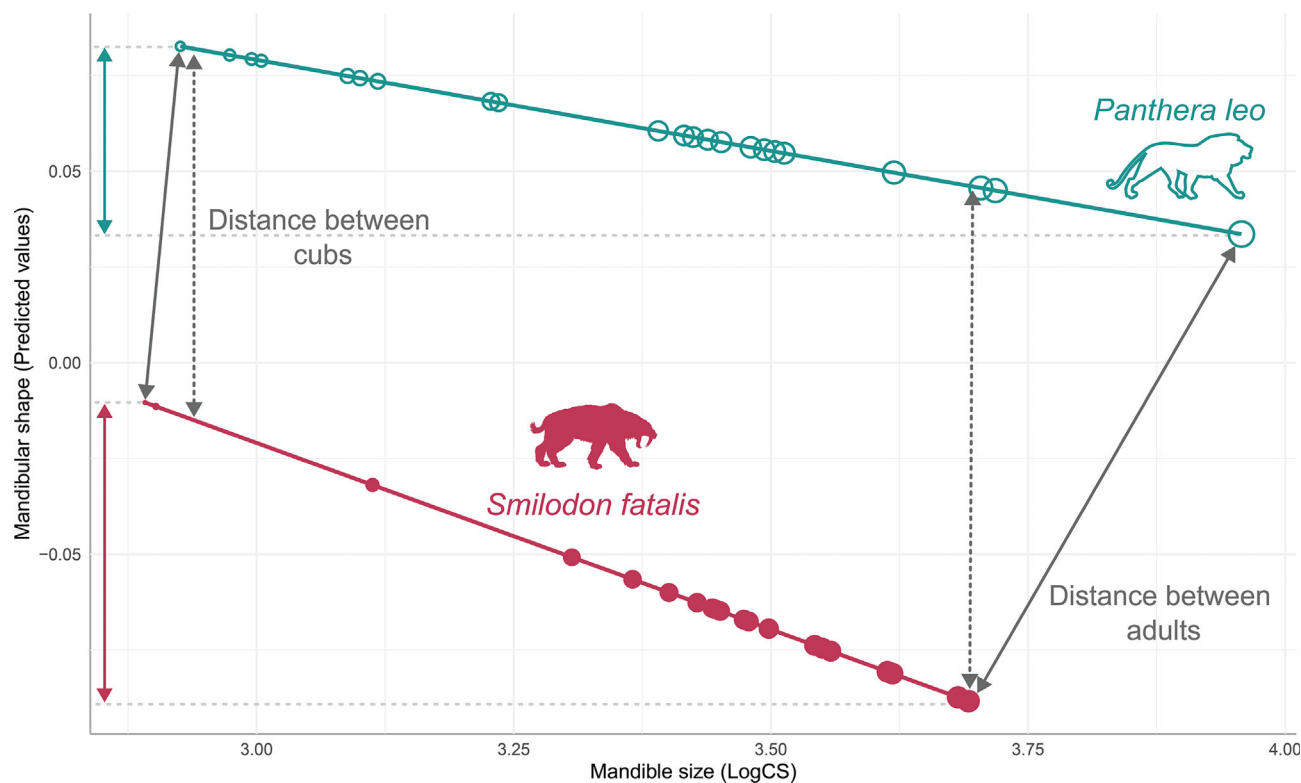


**FIGURE 7** Ontogenetic allometric trajectories with the first principal component of the predicted values of the multivariate regression of shape (Procrustes coordinates) on size plotted against the log-transformed centroid size for each mandible obtained from the plotAllometry function. Point size is relative to the log-transformed centroid size of each individual. Plane arrows highlight the distance between the smallest cubs and largest adults in both species while dotted arrows indicate the maximum distance between similar sized cubs and adults.

Although the height of the coronoid process and the length of the diastema show roughly similar trends (increasing with mandible length), the size allometry of those traits appear dissimilar in both species with marked differences in the slopes. The height of the coronoid process is quite small in both taxa (around 12 mm for cubs of *Smilodon* and 30 mm for lion cubs) but tends to develop much faster in *P. leo* than in *S. fatalis* ending at around 125 mm for the largest adult lion and barely reaching the size of the smallest lion cubs in adult *Smilodon* (Figure 8b, S3B and S4B), thereby creating a clear difference in slopes. The coronoid process of *S. fatalis* therefore does not show much change in absolute size, the main modification of this trait being the relative straightening (or verticalization) of this structure while it is more posteriorly projected in cubs. As for the diastema, smaller cubs in both species show relatively low values (8 mm for *P. leo* and 15 mm for *S. fatalis*) but the diastema length of *Smilodon* increases by 80% while *P. leo* shows a gentler linear increase with a shallow slope resulting in adult *S. fatalis* showing diastema length up to more than 70 mm whereas adult lions show a 70% increase toward 30 mm (Figure 8d, S3D, and S4D).

The most striking difference in our measurements is the variation of the angle of the symphysis region (a more vertical orientation of the symphysis being considered as a typical sabertooth trait). Small cubs in both taxa exhibit comparable values but while there is a clear declining trend in *S. fatalis* from 130° in the smallest cub to around 100° in adult specimens the angle distribution in lions appears somewhat random during growth, varying globally between 115° and 155° (Figure 8e, S3E and S4E).

### 3.5 | Functional variation during growth

Raw results of the FE simulations, computation of confidence intervals, standard deviations and final outputs can be found in Tables S6 and S7. We used three performance variables to compare the output from each model in our analyses: mechanical efficiency (ME), adjusted internal energy (adjIE), and the von Mises (VM) stress contour plots. Mechanical efficiency (Figure 9a) appears higher in cubs of *P. leo* than in cubs of *S. fatalis*. Juvenile lions with a mandibular length shorter than 120 mm

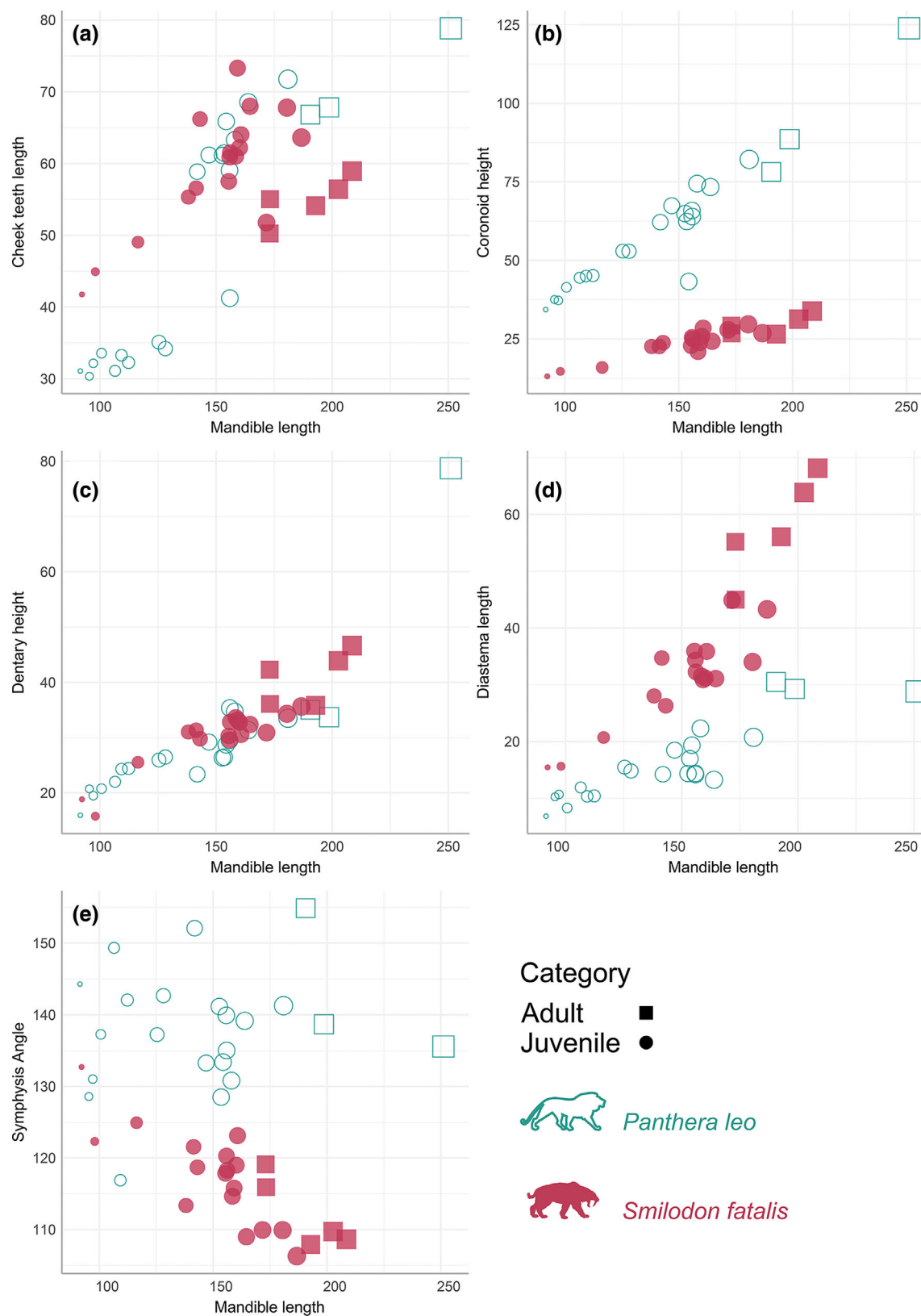


**FIGURE 8** Ontogenetic changes of linear and angular mandibular measurements taken in *Panthera leo* and *Smilodon fatalis* during growth: (a) cheek teeth length, (b) coronoid process height, (c) dentary height, (d) diastema length, and (e) symphysis angle. Squares represent adult individuals, circles represent juveniles. Point size is relative to the log-transformed centroid size of each individual.

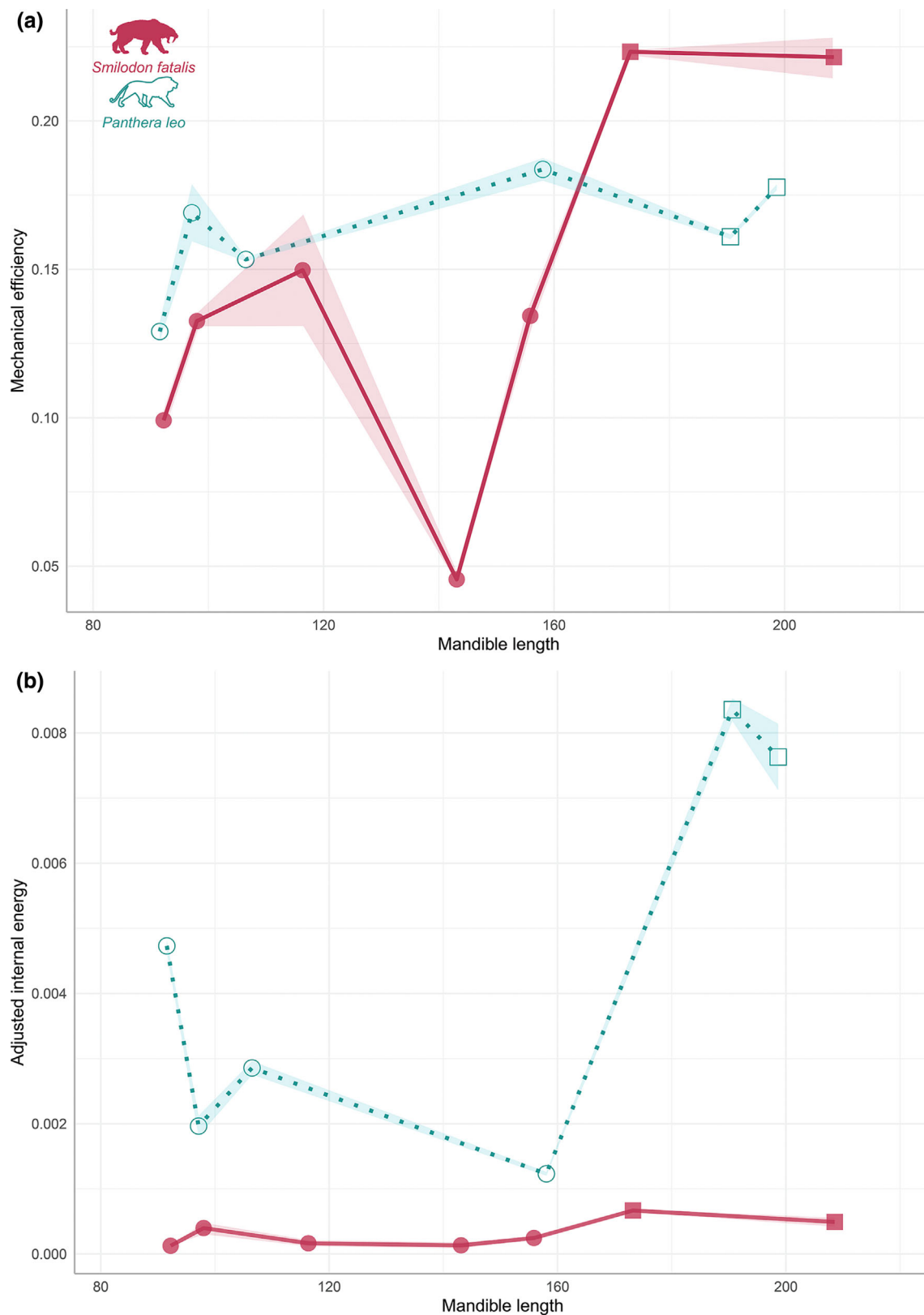


**FIGURE 9** Results of the anchor bite simulations on the mandibles: (a) mechanical efficiency and (b) adjusted internal energy with 95% confidence intervals. Mandible length is expressed in mm.

show a ME  $\sim 20\%$  higher than similarly-sized *Smilodon* (e.g. for a mandible length around 90 mm, ME for the juvenile lion = 0.13 while ME for the juvenile

*Smilodon* = 0.09, see Tables S6 and S7). This difference gets larger past 120 mm of mandibular length, with the ME of cubs of *S. fatalis* dropping to 0.04. However, larger



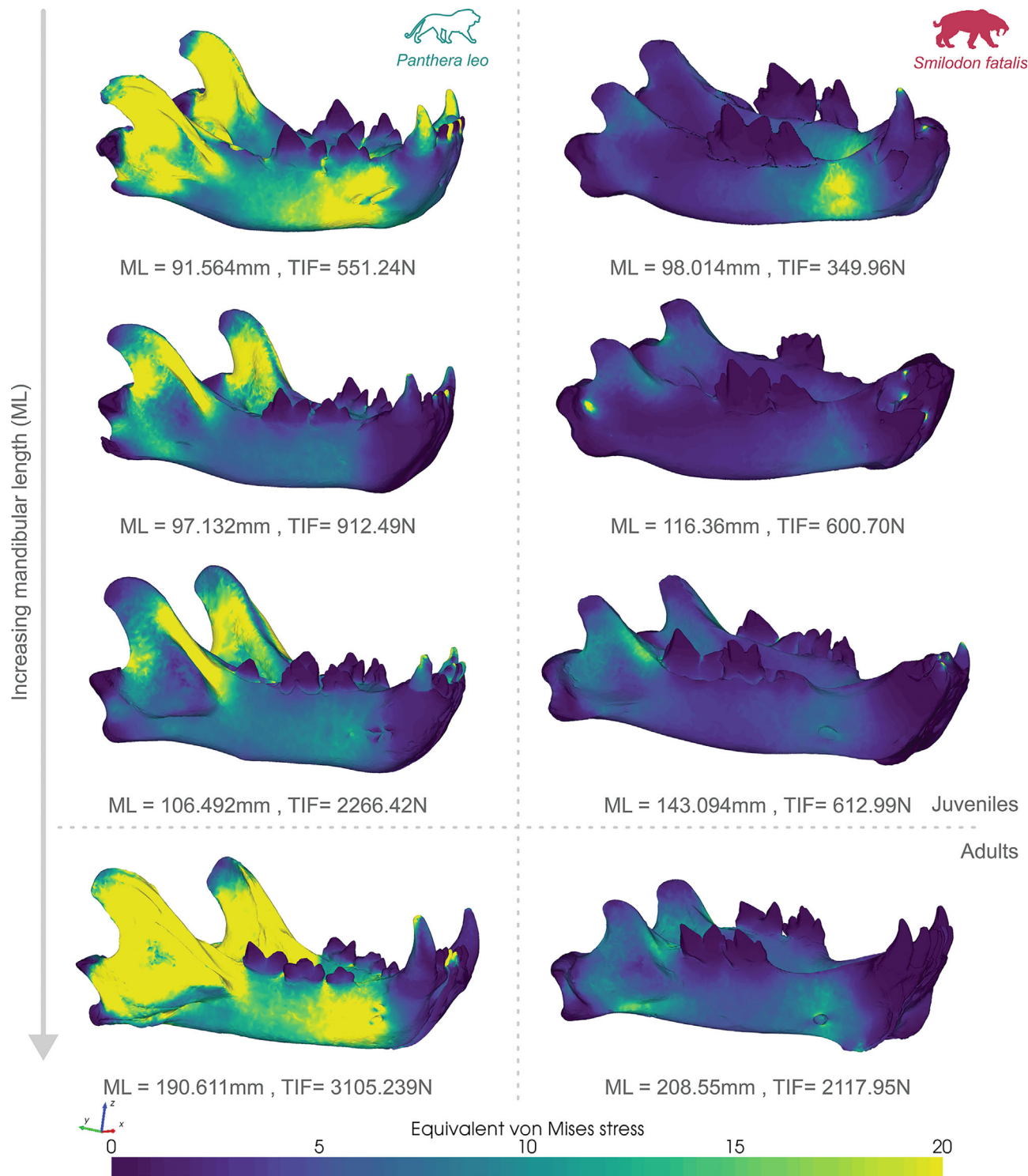


**FIGURE 10** von Mises stress contour plots on a subset of eight mandibles: *Panthera leo* on the left and *Smilodon fatalis* on the right with three juveniles and one adult in each species. Mandible length increases from top to bottom, VM stress varies from 0 to 20 MPa ( $\text{N}/\text{mm}^2$ ). Mandibles are not to scale, mandible length (ML) is expressed in mm and total input force (TIF) in N.

individuals of *Smilodon* show a drastic increase in ME exceeding those in the adult specimens of *P. leo*. The ME of our largest adult *Smilodon* reached as high as 0.23 while that of our largest adult lion barely reached 0.1888. Globally, the ME is relatively constant in the extant lion

varying with a 28% maximal variation: from 0.13 at its lowest (smallest cub, mandibular length = 91.56 mm) and up to 0.19 (large juvenile with a mandibular length of 158.04 mm). There is much more variation observed in *S. fatalis* with the lowest value of ME measured at 0.04 in

a mid-sized juvenile (mandibular length of 143.09 mm) while the highest ME value (0.23) was measured in our second largest adult specimen exhibiting a mandibular length of 208.55 mm resulting in an 81% increase.

Adjusted internal energy (Figure 9b) differs in magnitude between the two species: in *S. fatalis*, it varies from 0.00011 to 0.00063 (mJ/mm<sup>3</sup>) while in *P. leo* it is an order of magnitude higher, varying between 0.00119 and 0.00811. It is relatively high in the smallest cub but then drops at about 0.002, staying in between 0.002 and 0.003 until a mandible length of 180 mm where the adult specimens show a 700% increase of adjIE.

Von Mises stress contour plots (Figure 10) highlight a globally lower stress in *S. fatalis* than in *P. leo* during an anchor bite. There are large areas of high stress located in the coronoid process and diastema region in the smallest lion cub, the area of high stress in the diastema region then disappears in the larger cubs to finally re-appear in adult specimens. Adult lions exhibit particularly large areas of high stress during an anchor bite. Those observations are consistent with the evolution of the adjIE during the growth described above. In *S. fatalis*, there is an area of high stress located in the diastema region in the smallest cubs, which disappears in larger individuals. Stress then remains quite low, but areas containing the highest stress values are still located in the coronoid process and in the region of the diastema. This pattern is also observed in lions but remains below 10 MPa in *Smilodon* whereas it exceeds 20 MPa at any stage of mandibular development in *P. leo*.

## 4 | DISCUSSION

Our study of the ontogenetic changes in the mandible of *S. fatalis* aimed to quantify the change in shape throughout growth, potentially associated with dietary shifts and the development of the double fang phase. Additionally, we sought to compare the ontogenetic trajectories of *S. fatalis* with those of *P. leo* and further assess their biomechanical performances during growth. To identify potential variations in shape-performance relationships, the mandibular shape was quantified using 3D geometric morphometrics and linear morphometry across a dataset encompassing 49 mandibles. Subsequently, muscle-induced finite element simulations were conducted on a subset of 13 specimens, amounting to a total of 49 simulations.

We observed a clear mandibular shape shift in both the lion and *S. fatalis*, coinciding approximately with the eruption of the lower carnassial (Figure 5). According to (Smuts et al., 1978) the m1 can be felt through the gum at around 9 and 11 months in the extant lion. The end of the

weaning period is somewhat variable but occurs at about 10 months (Schaller, 1972) thus roughly coinciding with the eruption of m1. The eruption of the tooth entirely dedicated to cut meat allows the onset of the hypercarnivorous diet, and is associated with shifts in mandibular shape at this development stage as well: a straightening of the mandibular corpus and a rotation of the coronoid process, set more anteriorly. Those modifications make the mandible better suited to handle a more demanding food acquisition process by providing larger insertion zones for the masticatory muscles (masseter, temporalis), making the bite more powerful throughout ontogeny. This pattern of mandible development was previously reported in large felids such as the jaguar (*Panthera onca*), the puma (*Puma concolor*), and the cheetah (*Acinonyx jubatus*), as well as in medium-sized felids such as the bobcat (*Lynx rufus*) that can subdue prey that exceeds its size (Giannini et al., 2010; Segura, 2015). However, according to (Wysocki et al., 2015), *S. fatalis* had a delayed tooth eruption sequence compared with *P. leo*, meaning that it would also have a longer weaning period considering our results. A similar suggestion has been made by (Van Valkenburgh & Sacco, 2002), who proposed that *S. fatalis* may have required a delayed weaning period and longer maternal care until the adult dentition was fully functional. Estimating the age at which the adult dentition was fully functional is ambiguous, but recent studies suggest that the upper canines necessitated a particularly long time to fully erupt (up to 11 months) and that sub-adults of *S. fatalis* were double-fanged until an age of approximately 34–41 months (Wysocki et al., 2015). Within extant carnivores, there are different species that exhibit fairly large teeth, massive skulls, and considerable size, and which also show a remarkably long weaning period compared with other carnivores, for example, the brown hyaena (*Parahyaena brunnea*), the spotted hyaena (*Crocuta Crocuta*), and the polar bear (*Ursus maritimus*) (Bechshøft et al., 2008; Gittleman, 1986). Moreover, in addition to this longer weaning, *C. crocuta* does not achieve its full biomechanical potential until later in adulthood (Binder & Van Valkenburgh, 2000), which is similar to what we observe in our FE simulations on *S. fatalis*.

Results of our biomechanical simulations suggest that adult specimens of *S. fatalis* are better suited at handling an anchor bite than adult specimens of *P. leo* (Figure 10). However, it is interesting to note that this efficiency is acquired through ontogeny, as cubs of *S. fatalis* seem to be particularly inefficient (extremely low ME) to perform the anchor bite until a quite late age. A recent study by Reynolds et al. (Reynolds et al., 2021) on a remarkable assemblage of *S. fatalis* (two subadults approximately 2 years old found alongside an adult that was likely their mother) revived the debate about the potential social

interactions and parental care of *S. fatalis* which has always been controversial in the literature (Akersten, 1985; Carbone et al., 2009; Christiansen & Harris, 2012; Meachen-Samuels & Binder, 2010; Van et al., 2009; Van Valkenburgh & Sacco, 2002). The results of the two aspects we studied (shape and function) both suggest a prolonged parental care: shape shift at the eruption of the lower carnassial occurring later than in *P. leo* and a low biting efficiency of cubs of *Smilodon* until a quite late age.

According to some authors, the mandibular condyle might play a role in the “sabertooth killing bite.” The anatomy of this condyle in derived taxa such as *Smilodon* allowing a greater gape angle (Christiansen, 2011; Emerson & Radinsky, 1980). It was also noted by Chatar et al. (2021) that the size and shape of the mandibular condyle appear as a marked difference between extreme sabertoothed taxa and taxa with shorter upper canines: it is larger and inclined labially in sabertooths and smaller and inclined lingally in conical toothed cats. Christiansen (2012) mentioned that the mandibular condyle was more posteriorly displaced in derived sabertoothed taxa but still similar to felinae at the early stages of their development. In our dataset, it appears that juveniles show more developed mandibular condyles than in adult of the same species, the mandibular condyle remains quite well developed in *S. fatalis* while it is thin in adult specimens of *P. leo* relatively to the size of the mandible. This region could not be landmarked owing to an incomplete development in juvenile specimens but appears indeed as a region of dissimilar ontogenetic changes between *P. leo* and *S. fatalis*; the functional implications of those changes should be investigated in further studies.

Our analyses also highlight different ontogenetic trajectories between *P. leo* and *S. fatalis*. Marked differences that emerged between the smallest juveniles of both species include a coronoid process already quite short in *S. fatalis* and a diastema region already well-developed. Cubs of *S. fatalis* undergo more mandibular changes during growth particularly in the ascending ramus with a rotation of the coronoid process anteriorly, a greater lengthening of the diastema, a rotation of the symphyseal region posteriorly to a more vertical position, and the development of a small mental process, which is absent in the extant lion. Therefore, compared with the extant lion, the peculiar mandibular morphology of *S. fatalis* is the result of a combination of a dissimilar juvenile morphology but also of morphological changes exceeding those observed in extant felids. While this was already suggested for the cranial anatomy in another study, previous authors rather suggested that the juvenile mandibular anatomy of *Smilodon* was similar to that of adults (Christiansen, 2012). This assumption probably arose from a smaller sampling of mandibles compared with our

study. Reynolds et al. (2021) suggested that *S. fatalis* had a unique growth strategy, combining a fast growth, similar to what is observed in extant tigers (*Panthera tigris*), alongside prolonged parental care, similar to what is observed in *P. leo*. Those results are further corroborated by a previous study on carbon and oxygen isotopes within the enamel of upper canines also indicating that *S. fatalis* combined rapid growth and prolonged development over time (Feranec, 2004). Our results support this inference, considering both the highest slope of the ontogenetic trajectory of *S. fatalis* compared with *P. leo* and how *Smilodon* cubs/subadults were shown to be quite inefficient to perform an anchor bite. The evolution of some traits during growth differs in magnitude between the two species studied, e.g. the diastema region growth faster in *S. fatalis* than in *P. leo* while it is the opposite way around regarding the coronoid process (Figure 8) implying that these felids undergo different shape changes, affecting different areas of the mandible. The development of a mandibular flange is another example, unique to some sabertoothed taxa. While *S. fatalis* does not exhibit a developed flange like other machairodontines (e.g., *Megantereon* spp.) it still develops a small mental process, in adults. Some authors suggested that the acquisition of saberteeth in felids resulted in dramatic changes in the shape of the entire skull relative to felinae s.l (Christiansen, 2008) while others suggested that the sabertoothed cranial shape is the result of an exaggeration or co-opting of an allometric pattern of shape variation observed extant felids (Slater & Van Valkenburgh, 2009). Our data indicate that the mandible shape in adults *Smilodon* results from a combination of these two processes.

Finally, it is interesting to note that usually larger carnivorans exhibit higher stress and lower efficiency during biting simulations (see Tseng et al. (2017)). Thus, baseline allometric change is reflected in our dataset of *P. leo*, with juveniles showing lower stress values. However, the ontogenetic trajectory of *Smilodon* breaks this allometric trend by maintaining low internal energy and VM stress at different sizes, even in the largest adults. The latter might be consistent with the idea that the lower jaw has an anchoring function throughout ontogeny.

## 5 | CONCLUSIONS

Our analyses of mandibular shape and performance changes throughout ontogeny support the interpretation of a longer weaning period in *S. fatalis* than in extant felids, as well as a potentially prolonged period where adults would provide access to food. This inference is supported by the low efficiency of the juvenile mandible models to perform an anchor bite. Our results also



highlight different shape changes affecting different regions of the mandible in *S. fatalis* vs *P. leo*. However, it is also clear that the extreme morphology of adult *S. fatalis* was acquired as a combination of peculiar juvenile traits (e.g. short coronoid process) and stronger mandibular shape changes in specific regions such as the mandibular body. Although mandibles of *S. fatalis* exhibited higher efficiency than those of *P. leo* to perform an anchor bite, this efficiency is acquired quite late in ontogeny. The ontogeny of *Smilodon* does not follow the functional allometric trend usually observed in large carnivorans, by maintaining low internal energy and VM stress at the full ontogenetic range examined; this finding is consistent with the idea that the lower jaw has an anchoring function throughout ontogeny.

## AUTHOR CONTRIBUTIONS

**Narimane Chatar:** Conceptualization; data curation; formal analysis; funding acquisition; investigation; methodology; project administration; validation; visualization; writing – original draft; writing – review and editing. **Romain Boman:** Methodology; resources; software; writing – review and editing. **Valentin Fischer:** Conceptualization; resources; supervision; writing – review and editing. **Valentina Segura:** Conceptualization; investigation; writing – review and editing. **Clara Julémont:** Formal analysis; investigation. **Z. Jack Tseng:** Conceptualization; funding acquisition; investigation; methodology; supervision; writing – review and editing.

## ACKNOWLEDGMENTS

We are extremely thankful to all curators, collection managers and staff, whose help and support was fundamental to collect all the scans we needed to perform this study. Especially, we would like to thank: Geraldine Véron (MNHN, Paris, France), Emmanuel Gilissen (Royal Museum for Central Africa, Tervuren, Belgium), Aisling B. Farrell and Regan E. Dunn (La Brea tar pits museum, Los Angeles, USA), Jin Meng, Judith Galkin and Ruth O'Leary (AMNH, New York, USA), and finally Nicholas Pyenson, Amanda Millhouse and Matthew Miller (NMNH, Washington DC, USA). For their constructive comments about an earlier version of this work, we thank Anne Claire Fabre and Carlo Meloro. We thank Adam Harstone-Rose, Tahlia Pollock, and Lars Werdelin for the invitation to participate in the ICVM symposium leading to this special issue. Finally, we thank the three anonymous reviewers whose comments and suggestions helped building a stronger manuscript.

## FUNDING INFORMATION

Narimane Chatar was supported by a grant of Fonds de la Recherche Scientifique F.R.S.–FNRS (FRIA grant

number FRIA FC 36251) and is currently supported by a Belgian American Educational Foundation (BAEF) post-doctoral fellowship as well as a grant from the National Science Foundation (NSF DBI-2128146). VF was supported by a grant of Fonds de la Recherche Scientifique F.R.S.–FNRS (MIS F.4511.19). ZJT is supported by a grant from the National Science Foundation (DBI 2128146).

## DATA AVAILABILITY STATEMENT

3D models used to perform the analyses are available on Morphosource (Project ID: 000599525, <https://www.morphosource.org/projects/000599525>). Excel files containing the measurements, raw FE output for each specimen as well as the R script used to create the plots and perform the statistical tests are provided as supplementary files and are available on Orbi, the ULiège Open Repository (<https://hdl.handle.net/2268/318427>).

## ORCID

Narimane Chatar  <https://orcid.org/0000-0003-0449-8574>

Romain Boman  <https://orcid.org/0000-0002-4883-0383>

Valentin Fischer  <https://orcid.org/0000-0002-8808-6747>

Valentina Segura  <https://orcid.org/0000-0002-0307-4975>

Z. Jack Tseng  <https://orcid.org/0000-0001-5335-4230>

## REFERENCES

- Adams, D. C., & Otárola-Castillo, E. (2013). Geomorph: An R package for the collection and analysis of geometric morphometric shape data. *Methods in Ecology and Evolution*, 4, 393–399.
- Akersten, W. A. (1985). Canine function in *Smilodon* (Mammalia, Felidae, Machairodontinae). *Contributions in Science*, 356, 1–22.
- Alberch, P. (1980). Ontogenesis and morphological diversification. *American Zoologist*, 20, 653–667.
- Alberch, P., Gould, S. J., Oster, G. F., & Wake, D. B. (1979). Size and shape in ontogeny and phylogeny. *Paleobiology*, 5, 296–317.
- Anton, M. (2013). *Sabertooth*. Indiana University Press.
- Bechshøft, T., Sonne, C., Rigét, F. F., Wiig, Ø., & Dietz, R. (2008). Differences in growth, size and sexual dimorphism in skulls of East Greenland and Svalbard polar bears (*Ursus maritimus*). *Polar Biology*, 31, 945–958.
- Binder, W. J., Cervantes, K. S., & Meachen, J. A. (2016). Measures of relative dentary strength in rancho la brea *Smilodon fatalis* over time. *PLoS One*, 11, 1–9.
- Binder, W. J., & Van Valkenburgh, B. (2000). Development of bite strength and feeding behaviour in juvenile spotted hyenas (*Crocuta crocuta*). *Journal of Zoology*, 252, 273–283.
- Bookstein, F. (1991). *Morphometric tools for landmark data*. Cambridge University Press.
- Carbone, C., Maddox, T., Funston, P. J., Mills, M. G. L., Grether, G. F., & Van Valkenburgh, B. (2009). Parallels



- between playbacks and pleistocene tar seeps suggest sociality in an extinct sabretooth cat, *Smilodon*. *Biology Letters*, 5, 81–85.
- Chatar, N., Boman, R., Fallon Gaudichon, V., MacLaren, J. A., & Fischer, V. (2023). 'Fossils': A new, fast and open-source protocol to simulate muscle-driven biomechanical loading of bone. *Methods in Ecology and Evolution*, 14, 848–859.
- Chatar, N., Fischer, V., Siliceo, G., Antón, M., Morales, J., & Salesa, M. J. (2021). Morphometric analysis of the mandible of primitive Sabertoothed felids from the late Miocene of Spain Madrid. *Journal of Mammalian Evolution*, 28, 753–771.
- Chatar, N., Fischer, V., & Tseng, Z. J. (2022). Many-to-one function of cat-like mandibles highlights a continuum of sabre-tooth adaptations. *Proceedings of the Royal Society B: Biological Sciences*, 289, 20221627.
- Christiansen, P. (2007). Comparative bite forces and canine bending strength in feline and sabretooth felids: Implications for predatory ecology. *Zoological Journal of the Linnean Society*, 151, 423–437.
- Christiansen, P. (2008). Evolution of skull and mandible shape in cats (Carnivora: Felidae). *PLoS One*, 3, e2807.
- Christiansen, P. (2011). A dynamic model for the evolution of sabre-cat predatory bite mechanics. *Zoological Journal of the Linnean Society*, 162, 220–242.
- Christiansen, P. (2012). The making of a monster: Postnatal ontogenetic changes in craniomandibular shape in the great sabercat *Smilodon*. *PLoS One*, 7, e29699.
- Christiansen, P., & Harris, J. M. (2012). Variation in Craniomandibular morphology and sexual dimorphism in Pantherines and the Sabercat *Smilodon fatalis*. *PLoS One*, 7, e48352.
- Dessem, D., & Druzinsky, R. E. (1992). Jaw-muscle activity in ferrets, *Mustela putorius furo*. *Journal of Morphology*, 213(2), 275–286. <https://doi.org/10.1002/jmor.1052130211>
- Dixon, P. (2003). VEGAN, a package of R functions for community ecology. *Journal of Vegetation Science*, 14, 927–930.
- Eisenberg, J. F. (1981). *The mammalian radiations: An analysis of trends in evolution, adaptation, and behavior*. The University of Chicago Press.
- Emerson, S. B., & Radinsky, L. (1980). Functional analysis of sabertooth cranial morphology. *Paleobiology*, 6, 295–312.
- Erickson, G. M., Catanese, J., & Keaveny, T. M. (2002). Evolution of the biomechanical material properties of the femur. *Anatomical Record*, 268, 115–124.
- Feranec, R. S. (2004). Isotopic evidence of sabre-tooth development, growth rate, and diet from the adult canine of *Smilodon fatalis* from rancho La Brea. *Palaeogeography, Palaeoclimatology, Palaeoecology*, 206, 303–310.
- Giannini, N. P., Segura, V., Giannini, M. I., & Flores, D. (2010). A quantitative approach to the cranial ontogeny of the puma. *Mammalian Biology*, 75, 547–554.
- Gill, P. G., Purnell, M. A., Crumpton, N., Brown, K. R., Gostling, N. J., Stampanoni, M., & Rayfield, E. J. (2014). Dietary specializations and diversity in feeding ecology of the earliest stem mammals. *Nature*, 512, 303–305.
- Gittleman, J. L. (1986). Carnivore life history patterns: Allometric, phylogenetic, and ecological associations. *The American Naturalist*, 127, 744–771.
- Gould, S. J. (1985). *Ontogeny and phylogeny*. Harvard University Press.
- Grosse, I. R., Dumont, E. R., Coletta, C., & Tolleson, A. (2007). Techniques for modeling muscle-induced forces in finite element models of skeletal structures. *Anatomical Record*, 290, 1069–1088.
- Harris, J. M. (2015). In J. M. Harris (Ed.), *La Brea and beyond: The paleontology of asphalt-preserved biotas*. Natural History Museum of Los Angeles County.
- Hartstone-Rose, A., Long, R. C., Farrell, A. B., & Shaw, C. A. (2012). The clavicles of *Smilodon fatalis* and *Panthera atrox* (mammalia: Felidae) from rancho La Brea, Los Angeles, California. *Journal of Morphology*, 273, 981–991.
- Klein, R. G., & Cruz-Urbe, K. (1987). In L. Freeman & K. Butzer (Eds.), *The analysis of animal bones from archaeological sites*. The University of Chicago Press.
- Meachen-Samuels, J. A., & Binder, W. J. (2010). Sexual dimorphism and ontogenetic growth in the American lion and sabertoothed cat from rancho La Brea. *Journal of Zoology*, 280, 271–279.
- Merriam, J. C., & Stock, C. (1932). *The Felidae of rancho La Brea*. Carnegie Institution of Washington.
- Mitteroecker, P., Gunz, P., Bernhard, M., Schaefer, K., & Bookstein, F. L. (2004). Comparison of cranial ontogenetic trajectories among great apes and humans. *Journal of human evolution*, 46(6), 679–698. <https://doi.org/10.1016/j.jhevol.2004.03.006>
- Miller, G. J. (1968). On the age distribution of *Smilodon californicus* Bovard from rancho La Brea. *Contributions in Science*, 131, 1–17.
- R Core Team. (2021). *R: A language and environment for statistical computing*. R Core Team.
- Reynolds, A. R., Seymour, K. L., & Evans, D. C. (2021). *Smilodon fatalis* siblings reveal life history in a saber-toothed cat. *iScience*, 24, 24.
- Schaller, G. B. (1972). *The serengeti lion*. The University of Chicago Press.
- Segura, V. (2015). A three-dimensional skull ontogeny in the bobcat (*Lynx rufus*) (Carnivora: Felidae): A comparison with other carnivores. *Canadian Journal of Zoology*, 93, 225–237.
- Segura, V., Cassini, G. H., & Prevosti, F. J. (2017). Three-dimensional cranial ontogeny in pantherines (*Panthera leo*, *P. onca*, *P. pardus*, *P. tigris*; Carnivora: Felidae). *Biological Journal of the Linnean Society*, 120, 210–227.
- Slater, G. J., & Van Valkenburgh, B. (2009). Allometry and performance: The evolution of skull form and function in felids. *Journal of Evolutionary Biology*, 22, 2278–2287.
- Smuts, G. L., Anderson, J. L., & Austin, J. C. (1978). Age determination of the African lion (*Panthera leo*). *Journal of Zoology*, 185, 115–146.
- Stock, C. (1930). *Rancho La Brea: A record of Pleistocene life in California*. Los Angeles County Museum of Natural History.
- Stock, C., & Harris, J. M. (1992). *Rancho La Brea: a record of Pleistocene life in California* (7th edition). Natural History Museum of Los Angeles County.
- Stratovan Corporation. (2018). *Stratovan Checkpoint*. Stratovan Corporation.
- Tejada-Flores, A. E., & Shaw, C. A. (1984). Tooth replacement and skull growth in *Smilodon* from rancho La Brea. *Journal of Vertebrate Paleontology*, 4, 114–121.
- Tseng, Z. J. (2024). Bending performance changes during prolonged canine eruption in saber-toothed carnivores: A case study of *Smilodon fatalis*. *The Anatomical Record*. <https://doi.org/10.1002/ar.25447>

- Tseng, Z. J., Su, D. F., Wang, X., White, S. C., & Ji, X. (2017). Feeding capability in the extinct giant *Siamogale melilutra* and comparative mandibular biomechanics of living Lutrinae. *Scientific Reports*, 7, 1–10.
- Turner, A., Antón, M., Salesa, M. J., & Morales, J. (2011). Changing ideas about the evolution and functional morphology of Machairodontine felids. *Estudios Geológicos*, 67, 255–276.
- Van Valkenburgh, B., & Jenkins, I. (2002). Evolutionary patterns in the history of Permo-Triassic and Cenozoic synapsid predators. *The Paleontological Society Papers*, 8, 267–288.
- Van Valkenburgh, B., Maddox, T., Funston, P. J., Mills, M. G. L., Grether, G. F., & Carbone, C. (2009). Sociality in rancho La Brea *Smilodon*: Arguments favour 'evidence' over 'coincidence'. *Biology Letters*, 5, 563–564.
- Van Valkenburgh, B., & Sacco, T. (2002). Sexual dimorphism, social behavior, and intrasexual competition in large pleistocene carnivorans. *Journal of Vertebrate Paleontology*, 22, 164–169.
- VX model. 2023.
- Waddington, C. H. (1975). *The evolution of an evolutionist*. Edinburgh University Press.
- Werdelin, L., McDonald, H. G., & Shaw, C. A. (2018). In L. Werdelin, G. H. McDonald, & C. A. Shaw (Eds.), *Smilodon, the iconic sabertooth*. John Hopkins University Press.
- Wickham, H. (2016). ggplot2 (2nd ed.). Springer International Publishing. <https://doi.org/10.1007/978-3-319-24277-4>
- Wirkner, M., Heyder, K., & Ruf, I. (2022). Comparative morphology and postnatal ontogeny of the bony labyrinth in Pantherinae (Felidae, Carnivora) with special emphasis on the lion. *Vertebrate Zoology*, 72, 883–905.
- Wysocki, M. A., Feranec, R. S., Tseng, Z. J., & Bjornsson, C. S. (2015). Using a novel absolute ontogenetic age determination technique to calculate the timing of tooth eruption in the saber-toothed cat, *Smilodon fatalis*. *PLoS One*, 10, e0129847.

## SUPPORTING INFORMATION

Additional supporting information can be found online in the Supporting Information section at the end of this article.

**How to cite this article:** Chatar, N., Boman, R., Fischer, V., Segura, V., Julémont, C., & Tseng, Z. J. (2025). Growing sabers: Mandibular shape and biomechanical performance trajectories during the ontogeny of *Smilodon fatalis*. *The Anatomical Record*, 308(11), 2976–2993. <https://doi.org/10.1002/ar.25504>